RESEARCH PAPER

Controlled release of anticancer drugs via the magnetic magnesium iron nanoparticles modified by graphene oxide and polyvinyl alcohol: Paclitaxel and docetaxel

Ahmad Gholami [1], Biuck Habibi [1], Seyed Ali Hosseini [2], Amir Abbas Matin [3], Naser Samadi [4]*

[1]*Electroanalytical Chemistry Laboratory, Department of Chemistry, Faculty of Sciences, Azarbaijan Shahid Madani University, Tabriz 53714-161, Iran*
[2]*Department of Applied Chemistry, Faculty of Chemistry, Urmia University, Urmia, Iran*
[3]*Chromatogrphy Laboratory, Department of Chemistry, Faculty of Sciences, Azarbaijan Shahid Madani University, Tabriz 53714-161, Iran*
[4]*Analytical Spectroscopy Research Laboratory, Department of Chemistry, Faculty of Science, Urmia University, 1177, Urmia, Iran*

ABSTRACT

Objective(s): Paclitaxel (PTX) and docetaxel (DTX) belong to the family of taxanes drugs which have been employed for treatment of ovarian, breast, lung, head, neck, gastric, pancreatic, bladder, prostate and cervical cancer. Controlled drug release systems improve the effectiveness of drug therapy by modifying the release profile, biodistribution, stability and solubility, bioavailability of drugs and minimize the side effects of anticancer drugs. So, the purpose of the present study was to synthesize the modified nanocomposite for the controlled releases of these drugs.

Materials and Methods: Magnetic magnesium iron oxide nanoparticles were synthesized via the co-precipitation chemical method and then composited with graphene oxide and modified by polyvinyl alcohol. The physicochemical characterization of the prepared nanocomposites was investigated by scanning electron microscope (SEM), X-ray powder diffraction (XRD) , Fourier-transform infrared spectroscopy and vibrating-sample magnetometer.

Results: Specific characteristics such as adsorption capacity, monodispersity, stability and hydrophilicity of magnetic nanomaterials were studied in the controlled release of anticancer drugs. Drug loading content and drug loading efficiency and release rate of drugs were investigated in vitro at different pH with ultraviolet-visible spectroscopy (UV-Vis). DLE and DLC of PTX and DTX in the modified magnetic nanocomposites were calculated as 85.2 ± 2.7% and 7.74 ± 0.24% , 89.4 ± 1.2% and 8.12 ± 0.11% of, respectively. The cumulative release amount of PTX and DTX from magnetic modified nanocomposites at pHs 5.8, 7.4 over 100 h were 58 % and 40 % and 54 % and 37 %, respectively.

Conclusion: The potential of modified nanocomposite in drug delivery systems from the intrinsic properties of the magnetic core combined with their drug loading capability and the biomedical properties of modified nanocomposite generated by different surface coatings. The generally sustained and controlled release profile of DTX (or PTX) facilitates the application of modified nanocomposite for the delivery of anticancer drugs.

Keywords: *Anticancer drugs, Controlled drug release, Docetaxel, Graphene oxide, Magnetic magnesium iron nanoparticles, Polyvinyl alcohol, Paclitaxel*

How to cite this article
GholamiA, Habibi B, Matin AA, Samadi N. Controlled release of anticancer drugs via the magnetic magnesium iron nanoparticles modified by graphene oxide and polyvinyl alcohol: Paclitaxel and docetaxel. Nanomed J. 2021; 8(3): 200-210. DOI: 10.22038/NMJ.2021.57090.1584

INTRODUCTION

Among the substances that widely used in controlled drug delivery and drug release systems, magnetic nanoparticles are highly considered due to their unusual properties and ability to function at the cellular level of biological interactions [1-3]. The spinel magnetic magnesium ferrite oxide ($MgFe_2O_4$) nanoparticles (MMF NPs) is a soft magnetic nanomaterial that has received so far considerable attention in the medical and industrial fields, due to low toxicity, high specific surface area, biocompatibility, biodegradability,

* *Corresponding Author Email: B.Habibi@azaruniv.ac.ir; biuck-habibi_a@yahoo.com*
Note. This manuscript was submitted on April 6, 2021; approved on June 12, 2021

magnetic, electrical, optical, low hysteresis loss and high density properties [3-12]. On the other hand, graphene oxide (GO) with a unique structure that can be regarded as a single monomolecular layer of graphite with some oxygen-containing functionalities [13]. GO has a two-dimensional nanosheets structure as heavily decorated by oxygen-containing groups such as epoxide, carbonyl, carboxyl, and hydroxyl groups, which not only expand the interlayer distance but also make the atomic-thick layers hydrophilic as a result of which GO can be dispersed in several solvents like water [14, 15]. The large specific surface area of GO provides an ideal matrix for the growing and anchoring of MMF NPs or other functional substances to improve the adsorption capacity and prevents nanoparticles from aggregation [16, 17]. Integration of magnetic nanoparticles and GO as an adsorbent holds a great promise for a wide variety of applications in catalysis, removal of heavy metal ions and hazardous substances from aqueous solution, etc. [18]. Protection of magnetic nanoparticles (MNPs) and their composites is of prime importance for obtaining physically and chemically stable colloidal systems. Use of stabilizing surface coating materials may improve both the colloidal and physical stability of the particles, prevent both *in vitro* and *in vivo* agglomeration, increase their water-dispersibility, and provide functionalization for further conjugation with bioactive molecules or targeting ligands, and for obtaining multifunctional MNPs [19]. Utilizing polyvinyl alcohol (PVA) [20], as surface coating stabilizer for MNPs or composites, has the advantages of good aqueous dispersion and stability against oxidation of MNPs [21]. PVA has many uses such as adhesives, coatings, films, membranes, drug delivery systems and fuel cells, that have been applied in the industrial, commercial, medical, and food fields. PVA has been employed to increase the compactness and adhesion of GO coatings [22-25]. These compounds and their derivatives of water-soluble versions in particular are a suitable platform for development of efficient controlled drug delivery and release systems [26-30]. These nanocarriers can be loaded with drugs through non-covalent interactions or by covalent conjugation [31]. Conventional pharmacotherapy for the treatment of diseases leads to the occurrence of side effects and to the need for higher doses of the drug to elicit a satisfactory pharmacological response [32]. On the other hand, nanoparticles may consequently minimize the side effects and toxicity of the anticancer drugs while increase its therapeutic efficacy. Controlled drug release systems improve the effectiveness of drug therapy by modifying the release profile, biodistribution, stability and solubility, bioavailability of drugs and minimize the side effects of anticancer drugs. These methods reduce the number and quantity of drug dosages required during treatment and able to target specific sites in the body, thus optimize drug therapy [33, 34]. These systems for intravenous administration of drugs, able to evaluate the drug encapsulation efficiency, site specific treatments, regulate sustained drug release, extend drug retention time, reduce toxicity, and increase the half-life of drugs [35]. Nowadays, in cancer therapy and also treatment of other ailments, the controlled release of drugs by nanostructured functional materials especially MNPs is attracting increasing attention due to its opportunities. The intrinsic properties of the magnetic core of MNPs combined with their drug loading ability and the bio-chemical properties with a suitable coating show the potential of MNPs in the cancer therapy via controlled release of drugs [34]. The coated MNPs also show their potential applications in cancer hyperthermia (42-45°C) therapy. Drug delivery technology by MMF NPs-GO can be used to remove toxic and dangerous compound from the blood [36].

Paclitaxel (PTX) (sold under the brand name of Taxol) and docetaxel (DTX) or docetaxel Trihydrate (sold under the brand name of Taxotere) belong to the family of taxanes drugs which have been employed for treatment of ovarian, breast, lung, head, neck, gastric, pancreatic, bladder, prostate and cervical cancer. These drugs have traditionally been used in high doses every third week in the treatment of cancer as chemotherapeutic agents. These anticancer drugs involve the solvents cremophor and tween 80 which enhance the solubility of drugs, but cause high toxicity [37-40]. In recent years, it is noteworthy that that through targeted therapeutics, nanoparticle delivery systems have shown the potential to overcome the normal tissue toxicity of traditional chemotherapy. For example, nano-spheres of biodegradable polymers [41], PLGA/TPGS nanoparticles [42], poly(lactic acid)-poly(ethylene glycol)-poly(lactic acid) (PLA-PEG-PLA) microspheres [43], PNIPAAm-g-chitosan/PCL-Diol-b-PU core-shell nano-fibers

[44], PTX-Fe-BTC nanocomposite [45], poly(lactic acid)/hydroxyapatite core-shell nanoparticles [46] for paclitaxel, polyelectrolyte coated polymeric nanoparticles [47], PLA/PLGA nanoparticles [48], poly(lactic acid)/chitosan hybrid nanoparticles [49], polymeric nanoparticles [50], poly(3HB-*co*-4HB) biodegradable nanoparticles [51], PLGA nanoparticles[52] for docetaxel and chitosan-based advanced materials [53], N-(2-hydroxypropyl)methacrylamide (HPMA) copolymer [54] for both of them. In the present work, we report the synthesis of the magnetic magnesium ferrite oxide nanoparticles (MFO NPs) composited with GO and modified by PVA. Physicochemical characterizations of the prepared nanocomposites were investigated by different techniques and then were applied for controlled release of anticancer drugs; PTX and DTX.

MATERIALS AND METHODS

Materials

Sulphuric acid (98%), magnesium nitrate hexahydrate, iron (III) nitrate nonahydrate, iron (II) chloride tetrahydrate, iron (III) chloride hexahydrate and hydrogen peroxide (30%) were obtained from Sigma-Aldrich Company. Ammonia solution (28%), epychlorohydryne (ECH), sodium hydroxide, polyvinyl alcohol, ethanol, potassium permanganate ($KMnO_4$), hydrochloric acid (32% analytical grade), glutyrealdehyde and natural flake graphite (NFG) were obtained from Fulka Company. Taxol and taxotere were provided from the Urmia University of Medical Sciences and Tabriz University of Medical Sciences. The phosphate buffer solutions (PBS; 0.1 M) were made up of H_3PO_4, NaH_2PO_4, Na_2HPO_4, and $Na_3PO_4.7H_2O$ and adjusting the pH with of NaOH (1.0 M) or HCl (1.0 M) in order to obtain the desired pH value. All aqueous solutions are provided with deionized water. All experiments were conducted at ambient temperature (25 ± 2◦C).

Processes

Synthesis of magnetic Fe3O4 nanoparticles

Magnetic iron nanoparticles were synthesized from the alkaline solution of iron (II) and iron (III) salts by co-precipitation procedure. Iron (II) chloride tetrahydrate, $FeCl_2.4H_2O$, and iron (III) chloride hexahydrate, $FeCl_3.6H_2O$ were dissolved in water in a molar ratio of 1: 2 and was stirred for 15 min. To remove the dissolved oxygen disturbance, it was exposed to nitrogen and then ultrasonication for 20 min. Then the ammonia solution (3 M) was added dropwise until the pH reached 10 and stirring was continued for 1 h. The produced solid, Fe3O4 precipitate nanoparticles, was separated by a magnet and washed with ethanol.

Synthesis of magnetic $MgFe_2O_4$ nanoparticles

Magnetic $MgFe_2O_4$ nanoparticles (MFO NPs) were prepared by the co-precipitation procedure as reported earlier with some modification [55]. For the synthesis of the MFO NPs, a mixture of $Mg(NO_3)2.6H_2O$ (0.54 g, 2.1 mmol), $Fe(NO_3)_3.9H_2O$ (1.7g, 4.2 mmol), were dissolved in 50 ml distilled water and stirred. Next, NH_4OH (3 M) was added drop-wise in to this solution during 1 h at room temperature to obtain a mixture of pH=10 (to remove the dissolved oxygen disturbance, it was exposed to nitrogen gas). The produced solid, MFO NPs, was separated by a magnet and repeatedly washed with ethanol and deionized water to remove excess of ammonium and nitrate ions, and then dried at 100°C for 12 h in oven. The resulting sample was calcinated at 600°C for 8 h to evaluate the thermal stability and magnetic properties, and then grinded to obtain the fine nanoparticles.

Synthesis of graphene oxide

Graphene oxide (GO) was synthesized using the modified Hummer's method [56]. Briefly, 3.0 g graphite powder was slowly added in a concentrated H_2SO_4 (100 mL) solution in an ice bath. While maintaining vigorous stirring, 12.0 g (76 mmol) $KMnO_4$ and 3.0 g $NaNO_3$ were slowly added to the flask and the temperature was kept below 10°C. The mixture was stirred at ice bath for 1 h and then for another 1 h at 35°C. Deionized water (200 mL) was gradually added, causing an increase in temperature to 80-90°C and was stirred. After 15 min, the mixture was treated with 40 mL H_2O_2 (30 wt. %), which the color of the mixture changed to bright yellow (brown-colored viscous slurry). The mixture GO was centrifuged and washed with 1:10 HCl solution and deionized water for several times to remove the residual metal ions and the impurities until the pH was 7 and then dried at 65°C (at room temperature) in vacuum.

Preparation of the $MgFe_2O_4$-GO nanocomposite

25.0 mg GO was dispersed in 50 mL deionized water by sonication for 1 h. Then 0.15 g NaOH to transform the carboxylic acid groups to

carboxylate anions was added and stirred for 20 min. 5.0 ml epychlorohydryne (ECH) as coupling agent were added dropwise to GO solution at room temperature. After being ultrasonicated for 30 min and stirred for 30 min, 25.0 mg $MgFe_2O_4$ nanoparticles were added into the mixture, and stirred at 40°C for 12 h. The mixture was treated with ultrasonic device for 1 h. After the treatment, the $MgFe_2O_4$-GO nanocomposites were separated by centrifugation at 4000 rpm for 20 min and dried at room temperature under vacuum condition [57].

Preparation of $MgFe_2O_4$-GO nanocomposite modified by PVA

50.0 mg $MgFe_2O_4$-GO nanocomposite and 50 ml deionized water were treated with ultrasonic device for 1 h. Then 70.0 mg polyvinyl alcohol (PVA) was dissolved in 25 mL of water, which was slowly added dropwise into the mixture at room temperature with rapidly stirring for 20 min. (The mixture was heated for 6 h with constant stirring). Then 1 ml glutyrealdehyde and 1 ml HCl were added, and the mixture was sonicated for 30 min and stirred for 1 h. The modified nanocomposite, $MgFe_2O_4$-GO-PVA, were isolated by centrifugation at 4000 rpm for 20 min and washed twice with deionized water to remove free additional PVA and dried at room temperature under vacuum condition.

Paclitaxel loading on the $MgFe_2O_4$-GO-PVA modified nanocomposite

$MgFe_2O_4$-GO-PVA modified nanocomposite (100 mg) and a certain amount of paclitaxel (PTX) (10 mg) were dissolved in 5 ml mixture of ethanol and deionized water. The aliquot of the suspension was sonicated for 30 min and maintained under mechanical stirring for 24 h at 600 rpm. After the reaction, the $MgFe_2O_4$-GO-PVA modified nanocomposite as paclitaxel nanocarriers was separated by centrifuge at 4000 rpm for 20 min to remove the unloaded drugs and the supernatant was passed through membrane filter (pore size: 0.45 µm, Millipore). The resulting PTX loaded $MgFe_2O_4$-GO-PVA modified nanocomposite was cleaned by repeating the procedure of centrifuging and re-suspending in deionized water two times and then was collected with a laboratory magnet.

Docetaxel loading on the $MgFe_2O_4$-GO-PVA modified nanocomposite

$MgFe_2O_4$-GO-PVA modified nanocomposite (100 mg) and a certain amount of docetaxel (DTX) (10 mg) were dissolved in 5 ml mixture of ethanol and deionized water. The aliquot of the suspension was sonicated for 30 min and maintained under mechanical stirring for 24 h at 600 rpm. Then the mixture was centrifuged at 4000 rpm for 20 min to remove the unloaded drugs and the supernatant was passed through membrane. The resulting DTX loaded $MgFe_2O_4$-GO-PVA modified nanocomposite was cleaned by repeating the procedure of centrifuging and re-suspending in deionized water two times and then was collected with a laboratory magnet.

The drug content in the $MgFe_2O_4$-GO-PVA modified nanocomposite is defined as the ratio of the loaded drug to the total weight of solid magnetic nanocomposites. The loading efficiency is defined as the ratio of the loaded drug content to the total amount of drug used for nanocomposite preparation**.** In order to assess the drug concentration in the studied systems, UV-Vis measurements were utilized. PTX (or DTX) concentration was evaluated by the application of the Beer's law. By comparing UV spectra of supernatant and the standard calibration curve of absorbance maximum with concentration of DTX at λ max=229 nm and PTX at λ max= 231 nm, the amount of PTX (or DTX) adsorbed by the $MgFe_2O_4$-GO-PVA magnetic nanocomposite was measured.

The following equations were used to calculate

the drug loading efficiency (DLE) and drug loading content (DLC) [58]:

$$\text{Drug loading efficiency} = \frac{\text{weight of loaded drug in modified nanocomposite}}{\text{weight of initial loading of drug}} \times 100$$

$$\text{Drug loading content} = \frac{\text{weight of loaded drug in modified nanocomposite}}{\text{weight of PTX(or DTX)} - \text{modified nanocomposite}} \times 100$$

In vitro drug release study

PTX (or DTX) release experiments from solid magnetic modified nanocomposites was performed in phosphate buffered solution (PBS) medium (pH 5.8, 7.4) containing 0.5% Tween (or cremophor) at 37ºC, using the dialysis method. A weighed amount of DTX (or PTX) - loaded solid magnetic modified nanocomposites samples was re-suspended in PBS and then transported into a suitable dialysis bag. The dialysis bags were placed into 15 mL of pre-heated PBS as a release medium and shaken at at 37 ºC and 100 rpm, with the same pH. At certain time intervals, the solution outside of the dialysis bag was removed for UV–Vis analysis and replaced with an equal amount of fresh PBS solution. At fixed time intervals (e.g.

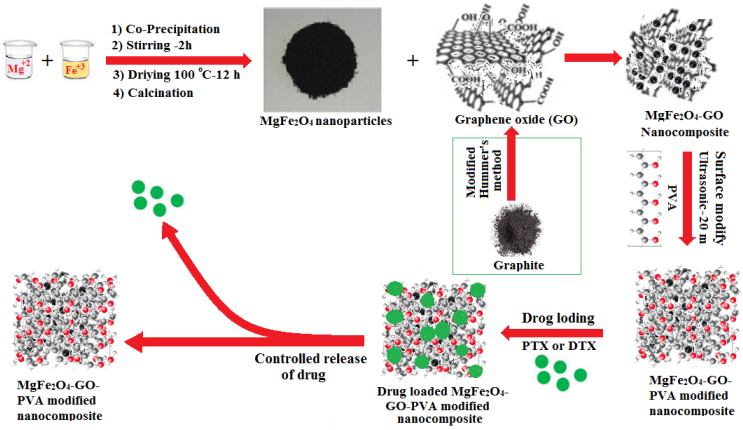

Scheme 1. Synthesis of the magnetic magnesium iron NPs modified by graphene oxide and polyvinyl alcohol

4 days) the amount of PTX (or DTX) released was monitored spectrophotometrically at 231 and 229 nm, respectively, and the amount of the released drug was calculated from a standard curve of free PTX (or DTX) solution. In the calculation of drug release behavior, the cumulative amount of released drug was calculated, and the percentages of released drug from solid magnetic modified nanocomposites were plotted against time. All experiments were carried out in triplicate. The results of triplicate measurements were used to calculate cumulative drug release [59, 60].

Instruments

Fourier-transform infrared spectroscopy (FT-IR); Thermo Scientific Ni-colet 95 IS10 FT-IR spectrometer, scanning electron microscope (SEM) and energy dispersive X-ray analysis (EDX); QUANTA 400F Field Emission SEM high-resolution scanning electron microscope, X-ray diffraction patterns (XRD); Brucker AXF (D8 Advance) X-ray powder diffractometer with a Cu Ka radiation source (λ = 0.154056 nm) generated at 40 kV and 35 mA, and vibrating sample magnetometer (VSM); Oxford type 1.2 T vibrating sample magnetometer analysis techniques were used for elemental analysis, size and surface morphology, structural analysis, and magnetic characterization of synthesized nanomaterials . All of the drug loading and release studies were analyzed using a Jenway UV-Visible Spectrophotometer (Model 6405).

RESULTS AND DISSCATION

The synthesis processes of the magnetic magnesium iron NPs modified by graphene oxide and polyvinyl alcohol are shown in scheme 1.

Physicochemical characterizations

FT-IR

In order to study the presence of functional groups in synthesized materials, FTIR analysis was carried out. FTIR spectra of the $MgFe_2O_4$ nanoparticles, $MgFe_2O_4$-GO nanocomposite and $MgFe_2O_4$-GO-PVA modified nanocomposite samples are presented in Fig 1. As shown in Fig 1 (spectrum a), the characteristic peaks at 438, 477 and 553 cm-1 for the $MgFe_2O_4$ nanoparticles are referred to the stretching vibrations of the octahedral and tetrahedral group complexes [61], which confirmed solid magnetic has spinel ferrites in structure, bending vibration of hydrogen-bonded surface water molecules is observed at 1637.52 cm^{-1} and broad absorption band at 3420 cm^{-1} is assigned to O-H stretching vibration [62]. The absorption peaks at 2363 cm^{-1} and 972 cm^{-1} are ascribed by the absorbed atmospheric CO_2 and formation of Mg substituted spinel ferrites [63]. The Fe-O characteristic stretching vibration peak at 568 cm^{-1} was observed in Fig 1. (spectrum

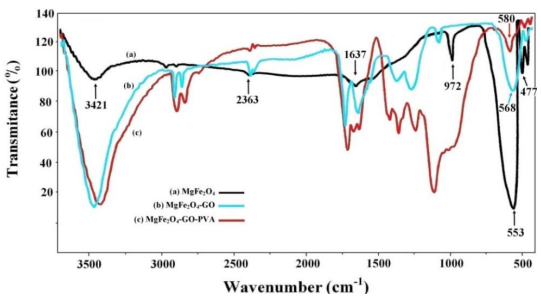

Fig 1. FT-IR spectra of $MgFe_2O_4$ nanoparticles (a), $MgFe_2O_4$-GO nanocomposite (b) and $MgFe_2O_4$-GO-PVA modified nanocomposite (c)

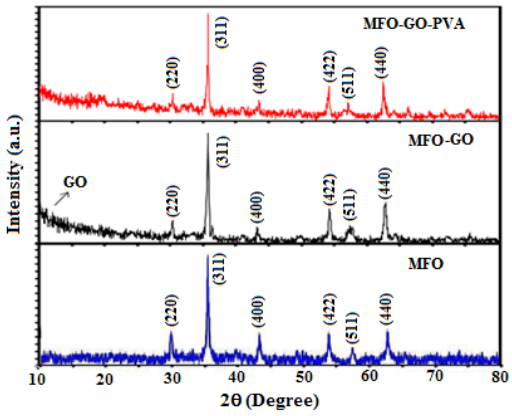

Fig 2. XRD patterns of $MgFe_2O_4$ nanoparticles (MFO), $MgFe_2O_4$-GO nanocomposite (MFO-GO) and $MgFe_2O_4$- GO-PVA modified nanocomposite (MFO-GO-PVA)

b), which proved that $MgFe_2O_4$ nanoparticles were successfully anchored onto GO sheet in the $MgFe_2O_4$-GO Fig 1: FT-IR spectra of $MgFe_2O_4$ nanoparticles (a), $MgFe_2O_4$-GO nanocomposite (b) and $MgFe_2O_4$-GO-PVA modified nanocomposite (c) nanocomposite [64]. But the absorption peak of the Fe-O vibration (580 cm^{-1}) decreased in Fig 1. (spectrum c), which suggested the encapsulation of MFO within the matrix of PVA in the $MgFe_2O_4$-GO-PVA modified nanocomposite [65].

XRD

X-ray diffraction (XRD) analysis was investigated for the study the structure and composition of synthesized materials. XRD patterns of $MgFe_2O_4$ nanoparticles, $MgFe_2O_4$-GO nanocomposite and $MgFe_2O_4$-GO-PVA modified nanocomposite were carried out in 2θ range of 10-80o. Fig 2. shows the XRD patterns of $MgFe_2O_4$ nanoparticles, $MgFe_2O_4$-GO nanocomposite and $MgFe_2O_4$-GO-PVA modified nanocomposite. As can be seen on the pattern of $MgFe_2O_4$ nanoparticles, the characteristic diffraction peaks were found at 30o, 35o, 43o, 53o, 57o, and 63 o that match well with data from the JCPDS card (88-1942) for $MgFe_2O_4$. These diffraction peaks corresponding to planes (220), (311), (400), (422),)511) and (440) provide a clear evidence for the formation of spinel structure of the magnetic magnesium ferrite nanoparticles [66]. The observed pattern is similar to literature and provides a clear evidence of $MgFe_2O_4$ formation [67, 68]. On the XRD patterns of the $MgFe_2O_4$-GO nanocomposite and $MgFe_2O_4$-GO-PVA modified nanocomposite same diffraction peaks were found which indicates that the crystallographic structure of the $MgFe_2O_4$ nanoparticles do not changed in the modification processes.

SEM

SEM images of $MgFe_2O_4$-GO nanocomposite and $MgFe_2O_4$-GO-PVA modified nanocomposite were carried out to know surface morphology and to estimate the particles size. Typical SEM images of $MgFe_2O_4$-GO nanocomposite and $MgFe_2O_4$-GO-

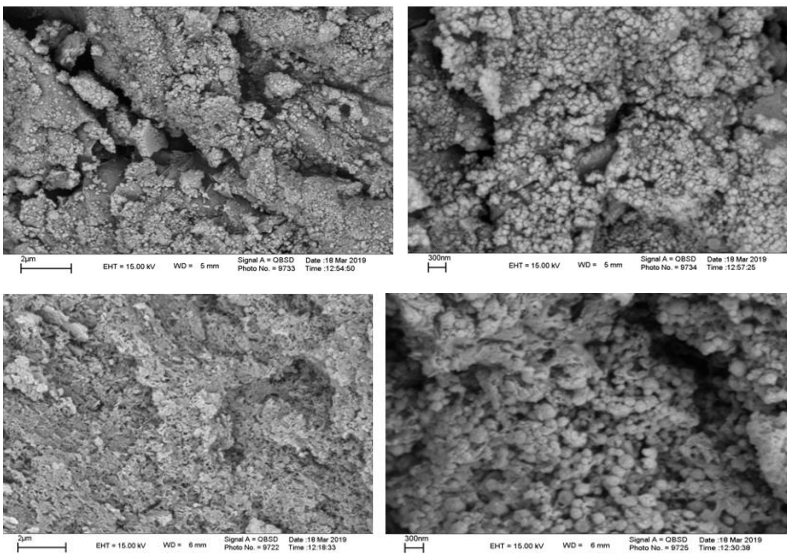

Fig 3. (up) SEM images of $MgFe_2O_4$-GO nanocomposite (two magnifications) and (down) SEM of $MgFe_2O_4$-GO-PVA modified nanocomposite (two magnifications)

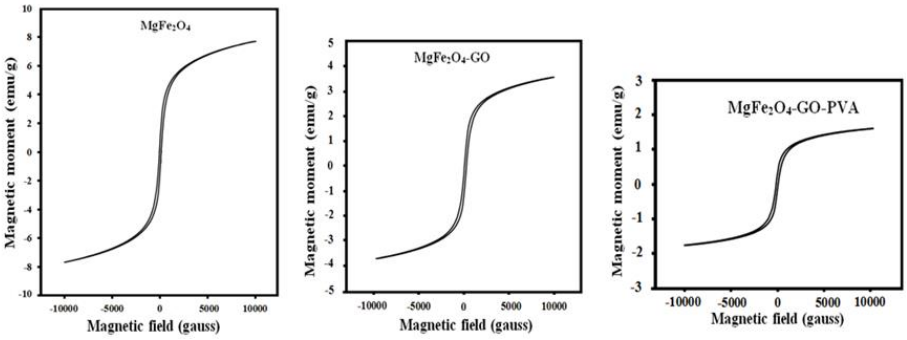

Fig 4. Magnetic hysteresis loops of (left) MgFe2O4 nanoparticles, (middle) $MgFe_2O_4$-GO nanocomposite and (right) $MgFe_2O_4$-GO-PVA modified nanocomposite

PVA modified nanocomposite are shown in Fig 3. (up) and (down), respectively. The images show the spherical morphology of the particles and the particles are uniformly wrapped by GO sheets and PVA. The estimated particle size was in the range of 40-70 nm. It was revealed by SEM imaging that the nanoparticles were generally spherical in shape with a narrow size distribution.

Vibrating-sample magnetometer (VSM) studies

Magnetization of $MgFe_2O_4$ nanoparticles demonstrated the clear s-shaped hysteresis loop that confirmed the ferromagnetic nature of $MgFe_2O_4$ nanoparticles. As shown in Fig 4. the saturation magnetization value (Ms) of $MgFe_2O_4$ nanoparticles (loop left) decreased with anchoring of MFO onto GO sheets nanocomposite (loop middle) and covering of nanocomposite with PVA (loop right) from 7.85 to 1.68 emu/g. The values of coercivity (Hc) increased with anchoring of MFO onto GO sheets and covering of nanoparticles with PVA from 98 to 204 Gauss. These results are presented in Fig 4. and Table 1.

Drug loading and in vitro drug release

In order to study of the drug release, the experiments were performed at the various dose of DTX (or PTX)-MFO-GO-PVA modified nanocomposite and pHs, so that the experiments had depending on time. The releasing of the drug were studied in the phosphate buffered medium in the range of times between 1 and 100 h. for this purpose 5, 10, 15 and 20 mg of DTX- MFO-GO-PVA modified nanocomposite and PTX- MFO-GO-PVA modified nanocomposite dose were used for studied of *in vitro* drug release. According to the Fig 5. with increasing the modified nanocomposite dose the concentration of loaded DTX and PTX increased [37-39]. Fig 6. revealed that the 10 mg dose had a gradual release in compared with 5, 15 and 15 mg of DTX- MFO-GO-PVA modified nanocomposite and PTX- MFO-GO-PVA modified nanocomposite. Due to the agglomeration of modified nanocomposite in 20 mg dose of DTX (or PTX)-MFO-GO-PVA modified nanocomposite and gradual release of the DTX and PTX drug in 10 mg,

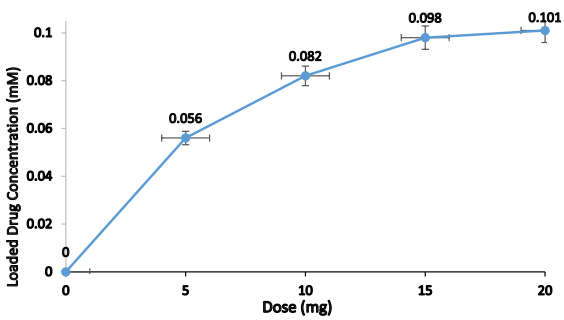

Fig 5. Loaded PTX and DTX Concentration (mM) in different doses of modified nanocomposite in PBS at 37 °C

Table 1. Various magnetic parameters for $MgFe_2O_4$ nanoparticles, $MgFe_2O_4$-GO nanocomposite and $MgFe_{2O}4$-GO-PVA modified nano-composite

Samples / Parameter	$MgFe_2O_4$	$MgFe_2O_4$-GO	$MgFe_2O_4$-GO-PVA
Magnetization (M_s) (emu/g)	7.85	3.73	1.68
Coercivity (H_c) (G)	98	148	204

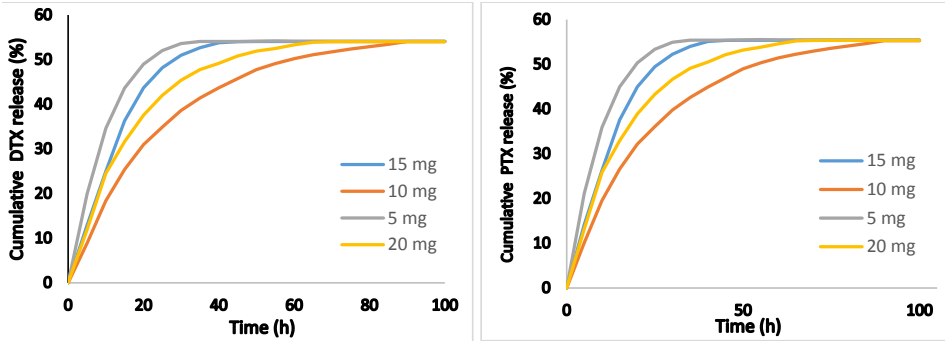

Fig 6. Cumulative release of DTX and PTX from modified nanocomposite immersed in PBS at different doses (5, 10, 15 and 20 mg) and 37°C

10 mg was specified as appropriate dose for this research. According to the Fig 6. in 5, 15 and 20 mg dose about 54% of DTX and PTX have released in less than 30 h. While in 10 mg dose of DTX- MFO-GO-PVA modified nanocomposite and PTX- MFO-GO-PVA modified nanocomposite 54% of the drug have released over the 85 h.

The *in vitro* drug release profiles of PTX- MFO-GO-PVA modified nanocomposite and DTX- MFO-GO-PVA modified nanocomposite in the 100h were investigated in PBS medium (pHs 7.4, 5.8) at 37°C in Fig 7. In the following 24 h, about 54 percent of PTX was released from MNPs at pH 5.8, compared with 58 percent of DTX, while about 37 percent of PTX was released from MNPs at pH 7.4, compared with 40 percent of DTX, respectively. After 100 h, the cumulative release amount of DTX from MFO-GO-PVA modified nanocomposite at pH 5.8 was only 58 % compared with 54 % of PTX, the cumulative release amount of DTX from MFO-GO-PVA modified nanocomposite at pH 5.8 over 100 h was only 58 %, compared with 54 % of PTX, respectively. As shown in Fig 5. the cumulative release of DTX (or PTX) was faster in acidic pH (pH 5.8) than in neutral pH (pH 7.4) [44].

Temperature has a great role in drug release and directly effects on the drug delivery process. The use of temperature as a bio-stimulant is considered due to the change in human body temperature in the presence of pathogens from the normal temperature of 37 °C. In order to study the effect of temperature the experiments were performed at temperature ranges from 10°C to 42°C. The results have shown in Fig 8. According to the Fig 8. drug cumulative drug release has increased by temperature increasing from 10 to 37 C but in the temperature ranges of 37°C to 43°C drug release significantly has decreased. The temperature effect on drug release may be attributed to both the reduction of PVA polymeric core stability in the bulk phase and the cell death at higher temperatures than 37°C [45].

The DTX (or PTX) loadings of MFO-GO-PVA modified nanocomposite were calculated and

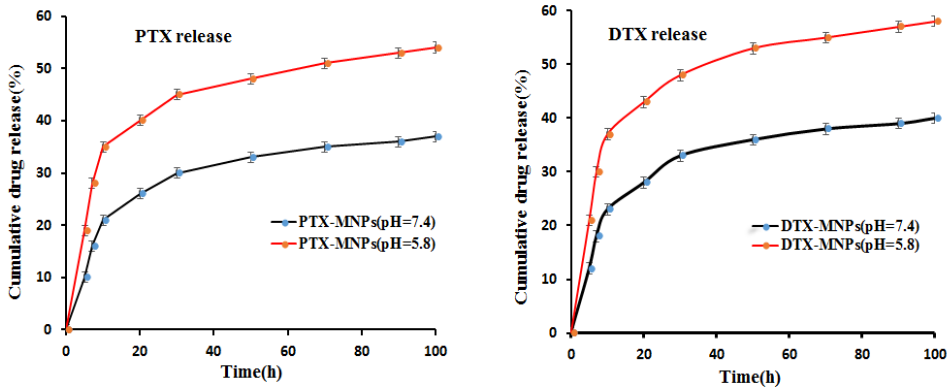

Fig 7. Cumulative release of PTX and DTX from modified nanocomposite immersed in PBS at different pH (7.4, 5.8) and 37°C

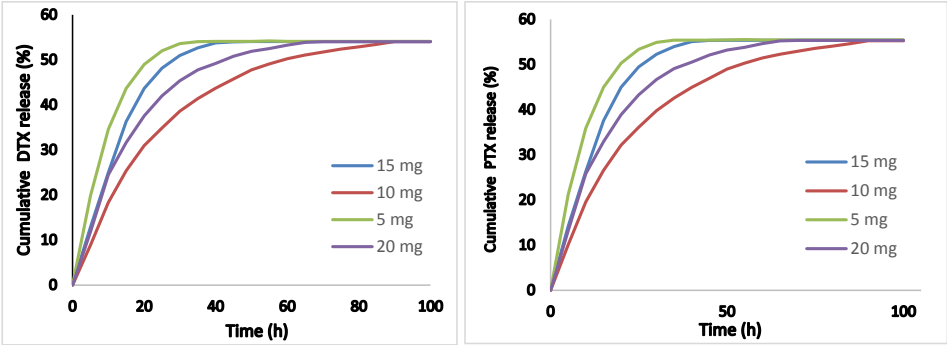

Fig 8. Cumulative release of PTX and DTX from modified nanocomposite immersed in PBS at different temperature (10-43 °C)

Tables 2. Calculated DLE and DLC of DTX (or PTX) for MFO-GO-PVA- modified nanocomposite

Drug Loading parameter	Docetaxel	paclitaxel
DLE	89.4 ± 1.2%	85.2 ± 2.7%
DLC	8.12 ± 0.11%	7.74 ± 0.24%

shown in Table 2. The result indicated that the DTX was effectively loaded into the modified nanocomposite, 89.4 ± 1.2% compared with 85.2 ± 2.7% of PTX. The DTX loading content of MFO-GO-PVA modified nanocomposite was 8.12 ± 0.11% w/w compared with 7.74 ± 0.24% of PTX.

CONCLUSIONS

$MgFe_2O_4$ nanocomposite with graphene oxide were fabricated via facile routes such as micro-emulsion and ultra-sonication route respectively. $MgFe_2O_4$ NPs were well anchored onto graphene oxide (GO) and the product was chemically modified with PVA successfully. The data of all characterizations techniques like XRD, FTIR, SEM and VSM were found in agreement with each other. XRD analysis reveals that the synthesized samples without trace of any impurity. The nano size of the $MgFe_2O_4$ powder, as observed from SEM image. The FTIR pattern confirms the characteristic peaks of ferrite system. The hysteresis loop exhibits ferromagnetic behavior. Utilizing GO shells and PVA coatings decrease the saturation magnetization value (Ms) of $MgFe_2O_4$ nanoparticles but increase coercivity (Hc) of nanocomposites. The potential of MFO-GO-PVA modified nanocomposite in drug delivery systems from the intrinsic properties of the magnetic core combined with their drug loading capability and the biomedical properties of MFO-GO-PVA modified nanocomposite generated by different surface coatings. The generally sustained and controlled release profile of DTX (or PTX) facilitates the application of MFO-GO-PVA modified nanocomposite for the delivery of anticancer drugs.

ACKNOWLEDGMENTS

The authors gratefully acknowledge the Research Council of Azarbaijan Shahid Madani University for financial support.

CONFLICTS OF INTEREST

There are no conflicts to declare.

REFERENCES

1. Xianbo M, Zeeshan A, Song L, Nongyue H. Applications of Magnetic Nanoparticles in Targeted Drug Delivery System. J Nanosci Nanotechnol. 2015; 15(1): 54-62.
2. Chomoucka J, Drbohlavova J, Huska D, Adam V, Kizek R, Hubalek J. Magnetic nanoparticles and targeted drug delivering. Pharmacol Res. 2010; 62(2): 144-149.
3. Gholami A , Mousavi SM, Hashemi SA, Ghasemi Y, Chiang WH, Parvin N. Current trends in chemical modifications of magnetic nanoparticles for targeted drug delivery in cancer chemotherapy. Drug Metab Rev. 2020; 52(1): 205-224.
4. Fernando R, Downs J, Maples D, Ranjan A. MRI-Guided Monitoring of Thermal Dose and Targeted Drug Delivery for Cancer Therapy. Pharm Res. 2013; 30: 2709-2717.
5. Reddy LH, Arias JL, Nicolas J, Couvreur P. Magnetic

nanoparticles: design and characterization, toxicity and biocompatibility, pharmaceutical and biomedical applications. Chemical Reviews. 2012; 112(11): 5818-5878.
6. Antic B, Jovic N, Pavlovic MB, Kremenovic A, Manojlovic D, Vasic MV, et al. Magnetization enhancement in nanostructured random type $MgFe_2O_4$ spinel prepared by soft mechanochemical route. J Appl Phys. 2010; 107(4): 043525.
7. Shahid M, Jingling L, Ali Z, Shakir I, Warsi MF, Parveen R, et al. Photocatalytic degradation of methylene blue on magnetically separable $MgFe_2O_4$ under visible light irradiation. Mater Chem Phys. 2013; 139(2-3): 566-571.
8. Yang G, Li X, Zhao Z, Wang W. Preparation, characterization, in vivo and in vitro studies of arsenic trioxide Mg-Fe ferrite magnetic nanoparticles. Acta Pharmacol Sin. 2009; 30: 1688-1693.
9. Khot VM, Salunkhe AB, Thorat ND, Ningthoujam RS, Pawar SH. Induction heating studies of dextran coated $MgFe_2O_4$nanoparticles for magnetic hyperthermia. Dal Trans. 2013;42:1249-1258.
10. Harish KN, Bhojya Naik HS, Prashanth Kumar PN, Viswanath R. Optical and photocatalytic properties of solar light active Nd-substituted Ni ferrite catalysts: for environmental protection. ACS Sustain Chem Eng. 2013; 9(1): 1143-1153.
11. Pan Y, Zhang Y, Wei X, Yuan C, Yin J, Cao D, et al.. $MgFe_2O_4$ nanoparticles as anode materials for lithium-ion batteries. Electrochim Acta. 2013; 109: 89-94.
12. Sepahvand R, Mohammadzadeh R. Synthesis and Characterization of Carbon Nanotubes Decorated with Magnesium Ferrite ($MgFe_2O_4$) Nanoparticles by Citrate-Gel Method. J Scie Islamic Rep Iran. 2011; 22(2): 177-182.
13. Dideikin AT, Vul AY. Graphene Oxide and Derivatives: The Place in Graphene Family. Front Phys. 2019; 6: 149-149.
14. Javed H, Rehman A, Mussadiq S, Shahid M, Azhar Khan M, Shakir I, et al.. Reduced graphene oxide-spinel ferrite nano-hybrids as magnetically separable and recyclable visible light driven photocatalyst. Synt Metals. 2019; 254: 1-9.
15. Marcano DC, Kosynkin DV, Berlin JM, Sinitskii A, Sun Z, Slesarev A, et al. Improved Synthesis of Graphene Oxide. ACS Nano. 2010; 8(4): 4806-4814
16. Rai AK, Gim J, Anh LT, Kim J. Partially reduced Co3O4/ graphene nanocomposite as an anode material for secondary lithium ion battery. Electrochim Acta. 2013; 100: 63-71.
17. Stankovich S, Dikin DA, Dommett GH, Kohlhaas KM, Zimney EJ, Stach EA, et al. Graphene-based composite materials. Nature. 2006; 442(20): 282-286.
18. Deng X, Lü L, Li H, Luo F. The adsorption properties of Pb(II) and Cd(II) on functionalized graphene prepared by electrolysis method. J Hazard mater. 2010; 183(1-3): 923-930.
19. Harivardhan Reddy L, Arias JL, Nicolas J, Couvreur P. Magnetic nanoparticles: design and characterization, toxicity and biocompatibility, pharmaceutical and biomedical applications.Chem Rev. 2012; 112(4): 5818-5878.
20. Moulay S. Review: Poly(vinyl alcohol) Functionalizations and Applications. Polym Plast Technol Eng. 2015; 54(12): 1289-1319.
21. Aisida SO, Ahmad I, Zhao Tk, Maaza M, Ezema FI. Calcination Effect on the Photoluminescence, Optical, Structural, and Magnetic Properties of Polyvinyl Alcohol Doped ZnFe2O4 Nanoparticles. J Macromol Sci B. Phys. 2020; 59(5): 295-308.
22. Mohsen-Nia M, Modarress H. Viscometric study of aqueous poly(vinyl alcohol) (PVA) solutions as a binder in adhesive formulations. J Adhes Sci Technol.2006; 20: 1273-1280.
23. Paradossi G, Cavalieri F, Chiessi E, Spagnoli C, Cowman MK. Poly(vinyl alcohol) as versatile biomaterial for potential biomedical applications. J Mater Sci: Mater Medi. 2003; 14(8): 687-691.
24. Musetti A, Paderni K, Fabbri P, Pulvirenti A, Al-Moghazy M, Fava P. Poly(vinyl alcohol)-Based Film Potentially Suitable for Antimicrobial Packaging Applications. J Food Sci. 2014; 79: E577-E582.
25. Hyon SH, Cha WI, Ikada Y, Kita M, Ogura Y, Honda Y. Poly(vinyl alcohol) hydrogels as soft contact lens material. J Biomater Sci, Poly E.1994; 5(5): 397-406.
26. Zhang J, Wang J, Lin T, Wang CH, Ghorbani K, Fang J, et al. Magnetic and mechanical properties of polyvinyl alcohol (PVA) nanocomposites with hybrid nanofillers - Graphene oxide tethered with magnetic Fe3O4 nanoparticles. Chem Eng J. 2014; 237: 462-468.
27. Qiu XP, Winnik F. Preparation and characterization of PVA coated magnetic nanoparticles. Chin J Poly Sci. 2000; 18: 535-539.
28. Kim SY, Ramaraj B, Yoon KR. Preparation and characterization of polyvinyl alcohol-grafted Fe3O4 magnetic nanoparticles through glutaraldehyde. Surf Inter Anal 2012; 44(9): 1238-1242.
29. Maleki A, Niksefat M, Rahimi J, Hajizadeh Z. Design and preparation of Fe3O4@PVA polymeric magnetic nanocomposite film and surface coating by sulfonic acid via in situ methods and evaluation of its catalytic performance in the synthesis of dihydropyrimidines. BMC Chem. 2019; 13: 19.
30. Mosiniewicz-Szablewska E, Clavijo AR, Castilho APOR, Paterno LG, Pereira-da-Silva MA, Więckowski J, et al. Magnetic studies of layer-by-layer assembled polyvinyl alcohol/iron oxide nanofilms. Phys Chem Chem Phys.2018; 20: 26696-26709.
31. Dobson J. Magnetic nanoparticles for drug delivery. Drug Develop Res. 2006; 67(1): 55-60.
32. Subramani K, Hosseinkhani H, Khraisat A, Hosseinkhani M, Pathak Y. Targeting Nanoparticles as Drug Delivery Systems for Cancer Treatment. Cur Nanosci. 2009; 5(2): 135-140.
33. Chomoucka J, Drbohlavova J, Huskab D, Adam V, Kizek R, Hubalek J. Magnetic nanoparticles and targeted drug delivering. Pharm Res. 2010; 62(2): 144-149.
34. Mukherjee S, Liang L, Veiseh O. Recent Advancements of Magnetic Nanomaterials in Cancer Therapy. Pharmaceutics 2020: 12(2): 147.
35. Swai H, Semete B, Kalombo L, Chelule P, Kisich K, Sievers B. Nanoparticulate alternatives for drug delivery. WIRES Nanomed Nanobio.2009; 1(3): 255-263.
36. Faraji A, Wipf P. Nanoparticles in cellular drug delivery. Bio Medi Chem. 2009; 17(8): 2950-2962.
37. Lin Z, Gao W, Hu H, Ma K, He B, Dai W, et al. Novel thermo-sensitive hydrogel system with paclitaxel nanocrystals: High drug-loading, sustained drug release and extended local retention guaranteeing better efficacy and lower toxicity. J Control Release. 2014; 174: 161-170.
38. Conte C, Ungaro F, Maglio G, Tirino P, Siracusano G, Sciortino MT, et al. Biodegradable core-shell nanoassemblies for the delivery of docetaxel and Zn(II)-phthalocyanine inspired by

combination therapy for cancer. J Control Release. 2013; 167(1): 40-52.
39. Kim SC, Kim DW, Shim YH, Bang JS, Oh HS, Kim SW, et al. In vivo evaluation of polymeric micellar paclitaxel formulation: toxicity and efficacy. J Control Release. 2001; 72 (1-3): 191-202.
40. Zhao P, Astruc D. Docetaxel Nanotechnology in Anticancer Therapy.ChemMedChem. 2012; 7: 952-972.
41. Feng SS, Huang G. Effects of emulsifiers on the controlled release of paclitaxel (Taxol®) from nanospheres of biodegradable polymers. J Control Release. 2001; 71(1): 53-69.
42. Mu L, Feng SS. PLGA/TPGS Nanoparticles for Controlled Release of Paclitaxel: Effects of the Emulsifier and Drug Loading Ratio. Pharm Res. 2003; 20: 1864-1872.
43. Ruan G, Feng SS. Preparation and characterization of poly(lactic acid)–poly(ethylene glycol)–poly(lactic acid) (PLA–PEG–PLA) microspheres for controlled release of paclitaxel. Biomater. 2003; 24(27): 5037-5044.
44. Farboudi A, Nouri A, Shirinzad S, Sojoudi P, Davaran S, Akrami M, et al. Synthesis of magnetic gold coated poly (ε-caprolactonediol) based polyurethane/poly(N-isopropylacrylamide)-grafted-chitosan core-shell nanofibers for controlled release of paclitaxel and 5-FU. Inter J Biolog Macromol. 2020; 150: 1130-1140.
45. Bikiaris ND, Ainali NM, Christodoulou E, Kostoglou M, Kehagias T, Papasouli E, et al. Dissolution Enhancement and Controlled Release of Paclitaxel Drug via a Hybrid Nanocarrier Based on mPEG-PCL Amphiphilic Copolymer and Fe-BTC Porous Metal-Organic Framework. Nanomater 2020; 10(12): 2490.
46. Lee S, Miyajima T, Sugawara-Narutaki A, Kato K, Nagata F. Development of paclitaxel-loaded poly(lacticacid)/hydroxyapatite core-shell nanoparticles as a stimuli -responsive drug delivery system. R Soc Open Sci. 2021; 8: 202030.
47. Agrawal R, Shanavas A, Yadav S, Aslam M, Bahadur D, Srivastava R. Polyelectrolyte Coated Polymeric Nanoparticles for Controlled Release of Docetaxel. J Biomed Nanotechnol. 2012; 8(1): 19-28.
48. Musumeci T, Ventura CA, Giannone I, Ruozi B, Montenegro L, Pignatello R, et al. PLA/PLGA nanoparticles for sustained release of docetaxel. Inter J Pharm. 2006; 325(1-2): 172-179.
49. Wang W, Chen S, Zhang L, Wu X, Wang J, Chen JF, et al. Poly(lactic acid)/chitosan hybrid nanoparticles for controlled release of anticancer drug. Mater Sci Eng: C. 2015; 46: 514-520.
50. Karimi N, Soleiman-Beigi M, Fattahi A. Co-delivery of all-trans-retinoic acid and docetaxel in drug conjugated polymeric nanoparticles: Improving controlled release and anticancer effect. Mater Today Commun. 2020; 25: 101280.
51. Faisalina AF, Sonvico F, Colombo P, Amirul AA, Wahab HA, Abdul Majid MI. Docetaxel-Loaded Poly(3HB-co-4HB) Biodegradable Nanoparticles: Impact of Copolymer Composition. Nanomater 2020; 10(11): 2123.
52. Wang X, Cheng R, Zhong Z. Facile fabrication of robust, hyaluronic acid-surfaced and disulfide-crosslinked PLGA nanoparticles for tumor-targeted and reduction-triggered release of docetaxel. Acta Biomater. 2021; 125(15): 280-289.
53. Ashrafizadeh M, Ahmadi Z, Mohamadi N, Zarrabi A, Abasi S, Dehghannoudeh G, et al. Chitosan-based advanced materials for docetaxel and paclitaxel delivery: Recent advances and future directions in cancer theranostics. Inter J Biolog Macromol. 2020; 145: 282-300.
54. Etrych T, Šírová M, Starovoytova L., Říhová B Ulbrich, K. HPMA Copolymer Conjugates of Paclitaxel and Docetaxel with pH-Controlled Drug Release. Molecul Pharm. 2010; 7(4): 1015-1026.
55. Ali R, Khan MA, Mahmood A, Chughtai AH, Sultan A, Shahid M, et al. Structural, magnetic and dielectric behavior of Mg1−xCaxNiyFe2−yO4 nano-ferrites synthesized by the micro-emulsion method. Ceram Inter. 2014; 40(3): 3841-3846.
56. Hummers WS, Offeman RE. Preparation of Graphitic Oxide. J Am Chem Soc. 1958; 80(6): 1339-1339.
57. Shakir I, Sarfraz M, Ali Z, Aboud MFA, Agboola PO. Magnetically separable and recyclable graphene-$MgFe_2O_4$ nanocomposites for enhanced photocatalytic applications. J Alloy Comp. 2016; 660: 450-455.
58. Tarhan T, Tural B, Tural S. Synthesis and characterization of new branched magnetic nanocomposite for loading and release of topotecan anti-cancer drug. J Anal Sci Tech. 2019; 30(10): 1-13.
59. Feng S-S, Mei L, Anitha P, Gan CW, Zhou W. Poly(lactide)–vitamin E derivative/montmorillonite nanoparticle formulations for the oral delivery of Docetaxel. Biomater. 2009; 30(19): 3297-3306.
60. Yin Y-M, Cui F-D, Mu C-F, Choi M-K, Kim JS, Chung S-J, et al. Docetaxel microemulsion for enhanced oral bioavailability: preparation and in vitro and in vivo evaluation. J Control Release. 2009; 140(2): 86-94.
61. Zhou H, Hu L, Wan J, Yang R, Yu X, Li H, et al. Microwave-enhanced catalytic degradation of p-nitrophenol in soil using $MgFe_2O_4$. Chem Eng J. 2016; 284: 54-60.
62. Nguyen LTT, Nguyen LTH, Manh NC, Quoc DN, Quang HN, Nguyen HTT, et al. A Facile Synthesis, Characterization, and Photocatalytic Activity of Magnesium Ferrite Nanoparticles via the Solution Combustion Method. J Chem. 2019; 2019:Article ID 3428681.
63. Reddy MP, Zhou XB, Huang Q, Ramakrishna Reddy R. Synthesis and Characterization of Ultrafine and Porous Structure of Magnesium Ferrite Nanospheres. Inter J Nano StudTechnol. 2014; 3(6): 72-77.
64. Chandradass J, Jadhav AH, Kim KH, Kim H. Influence of processing methodology on the structural and magnetic behavior of $MgFe_2O_4$ nanopowders. J Alloy Compounds. 2012; 517: 164-169.
65. Nasar G, Magnesium ferrite/polyvinyl alcohol (PVA) nanocomposites: Fabrication and characterization. J Nanomater Mol Nanotechnol. 2019;DOI: 10.4172/2324-8777-C4-065.
66. Zheng L, Fang K, Zhang M, Nan Z, Zhao L, Zhou D, Zhu M, Li W. Tuning of spinel magnesium ferrite nanoparticles with enhanced magnetic properties. RSC Adv. 2018; 8: 39177-39181.
67. Li YF, Liu YZ, Zhang WK, Guo CY, Chen CM. Green synthesis of reduced graphene oxide paper using Zn powder for supercapacitors. Mater Let. 2015; 157: 273-276.
68. Rai AK, Thi TV, Gim J, Kim J. Combustion synthesis of $MgFe_2O_4$/graphene nanocomposite as a high-performance negative electrode for lithium ion batteries. Mater Charact. 2014; 95: 259-265.